A comparative study of the roles of KCN and NaCN as catalytic precursors in the Boudouard reaction

M. Alam and T. DebRoy

Department of Materials Science and Engineering, The Pennsylvania State University, University Park, PA 16802, USA

The rate of reaction between carbon dioxide and coke with or without added KCN and NaCN was studied using thermogravimetry. The chemical stability of KCN or NaCN during catalysis, the changes in the concentration of potassium or sodium in coke and the pore structure of coke were studied as a function of time. The influences of these variables on the rate of coke–CO_2 reaction were determined. Since the catalysis depends on the catalyst carbon contact, the distribution of potassium in the coke structure was examined. A porous solid reaction model was used to examine the contributions of chemical reaction and pore diffusion in the overall rate of coke–CO_2 reaction.

The effect of inorganic impurities on the kinetics of gasification of carbonaceous materials with CO_2 has been the subject of intensive investigation in the past[1-3]. Alkali metal oxides[4-5], hydroxides[6-8], cyanides[9-10], cyanates[10] and carbonates[4-6,10-12] are among the most active catalytic precursors for the carbon–CO_2 reaction. This is due to the fact that these compounds are either easily converted to an elemental form or transformed to compounds that are intermediate products in the gasification of carbon.

Various alkali metal compounds are commonly present in a number of metallurgical and chemical reactors. In this study, the roles of KCN, KOCN, K_2CO_3 and NaCN on the coke–carbon dioxide reaction were studied. It was therefore possible to examine the effects of both anionic and cationic constituents of the precursors in the catalysis and obtain useful information about the mechanism of catalysis.

In the absence of a catalyst in coke, the rate of diffusion of CO_2 through the gas boundary layer and the porous coke is often faster than the rate of the intrinsic chemical reaction between coke and CO_2[13]. However, when a catalyst is added to the coke, the rate of the chemical reaction is dramatically enhanced[1-3]. Thus, the diffusion process becomes relatively more important and the role of structural parameters such as the porosity and pore size distribution become vital in determining the rate of the reaction. Therefore, an understanding of the structural effects in the catalytic reaction between CO_2 and coke is central to an understanding of the roles of the catalytic precursors in the solution loss reaction.

The rate of reaction between coke and carbon dioxide was studied by thermogravimetry. The changes in the chemical nature of the potassium- and sodium-bearing compounds added to coke were examined by X-ray diffraction analysis. The changes in the concentration of potassium and sodium in the coke samples doped with various catalytic precursors were determined by atomic absorption spectroscopy. The structural changes of the coke were monitored by measuring both its specific surface area by the nitrogen adsorption technique, and its pore structure as a function of the extent of reaction by mercury porosimetry and scanning electron microscopy. The distribution of potassium in the coke structure was examined by the energy dispersion X-ray technique. From an analysis of the rate data and information about the structural changes, the contribution of pore diffusion to the overall rate was determined using a structural model.

EXPERIMENTAL

Sample preparation

The proximate and ultimate analyses and the ash composition of the coke are given in *Table 1*. The coke had a reactivity of 17.1 % on the Bethlehem scale[14]. The coke was pulverized and the fraction $-270+325$ mesh (45–53 μm) thoroughly mixed with KCN or NaCN using a pestle and mortar and discs of 9.5×10^{-3} m diameter and 4.75×10^{-3} m thickness were then pressed under a 3.52×10^5 kg load. A small amount of deionized water was used as a binder. The bulk density of the pellets was $\approx 1.5 \times 10^3$ kg m^{-3}.

Thermogravimetry

The thermogravimetric set-up consisted of a Cahn microbalance (Model 1000, 0.50 μg sensitivity) and a high temperature silicon carbide vertical tube furnace with a 0.025 m long equi-temperature zone at the centre. The temperature was regulated by a Eurotherm controller to an accuracy of ± 2 K. The gas purification train had provisions for the removal of moisture, hydrocarbons, O_2, CO and CO_2 from argon. Similarly, moisture,

Table 1 Proximate and ultimate analyses and ash composition of experimental coke

Proximate analysis (wt %)	
Fixed carbon	93.5
Volatiles	2.0
Moisture	0.3
Ash	5.5
Ultimate analysis (wt %, dry composition)	
Carbon	92.1
Hydrogen	0.2
Nitrogen	1.3
Sulphur	0.6
Ash composition	
SiO_2	53.2
Al_2O_3	22.3
Fe_2O_3	14.4
TiO_2	2.7
K_2O	1.7
MgO	0.8
CaO	0.7
Na_2O	0.08
Cr_2O_3	0.07

hydrocarbons and CO were removed from CO_2 , while CO was cleaned to eliminate moisture, hydrocarbons and CO_2.

The coke pellet was placed in a platinum wire basket and suspended from one arm of the Cahn balance with a 0.005 m diameter platinum wire. The system was first purged with argon flowing at a rate of 8.3×10^{-6} m³ s⁻¹ at 298 K and 101.3 KPa total pressure for 30 min. The furnace was then heated to 473 K for the removal of moisture from the sample. After moisture removal, indicated by a constant sample weight on a strip chart recorder, the furnace temperature was raised to the reaction temperature (1123 K). The furnace heating rate was kept constant for all runs. After reaching the desired temperature, the flow rates of the reacting gases were adjusted to the required values.

Identification of the alkali compounds and concentrations of the alkali metals

A Rigaku X-ray diffractometer was used for identification of the potassium and sodium salts in the partially reacted coke samples. A Perkin Elmer Model 703 atomic absorption spectrophotometer was used to determine the changes in the concentration of potassium and sodium in the coke samples.

Coke structure and potassium

The structure of the coke samples was characterized with regard to specific surface area, pore size distribution, porosity and mean pore radius.

The specific surface area of the coke was determined by N_2 adsorption and the BET treatment of the adsorption isotherms. A Quantasorb Sorption System was used with helium as the carrier gas.

The pore size distribution, porisity and average pore radius of the coke were determined by mercury intrusion technique using an AMINCO (1.034×10^5 KPa) digital read out porosimeter. The unit was capable of determining the equivalent pore radius from 50 to 0.012 μm (assuming 130° contact angle).

The microstructural changes of the coke samples were examined by scanning electron microscopy. The distribution of potassium in the coke structure was examined by the energy dispersion X-ray technique.

RESULTS AND DISCUSSION

Chemical stability of catalytic precursors

The alkali metal cyanides added to the coke may react with CO_2 during coke gasification. The following reactions can occur:

$$2MCN + 4CO_2 = M_2CO_3 + 5CO + N_2 \tag{1}$$
$$MCN + CO_2 = MOCN + CO \tag{2}$$
$$2MOCN + 2CO_2 = M_2CO_3 + 3CO + N_2 \tag{3}$$
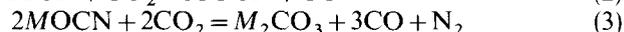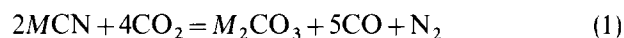
$M = K$ or Na. All the above reactions are thermodynamically feasible in pure CO_2 at 1123 K. Thus, MCN may be partially converted to $MOCN$ or M_2CO_3 while $MOCN$ may form M_2CO_3. To examine the reaction between the KCN present in coke and CO_2, a sample weighing 8.5×10^{-4} kg and containing coke and KCN in the weight ratio of 1:1 was reacted with pure CO_2 at 1123 K until 25 % of the initial weight of the sample was lost. The partially reacted sample was subsequently analysed by X-ray diffraction which indicated the presence of KOCN and KCN.

K_2CO_3 could not be identified in the X-ray analysis of the partially reacted KCN doped sample. However, its presence was determined by wet chemical analysis. A sample containing coke and KOCN was also reacted with pure CO_2 to examine the feasibility of Reaction (3). The partially reacted sample was then analysed by X-rays and the results indicated that KOCN indeed reacted with CO_2 to form K_2CO_3.

Similar experiments were carried out to examine the reaction between NaCN and NaOCN with CO_2. The data indicated that the NaCN present in coke reacts with CO_2 to form NaOCN and Na_2CO_3 while NaOCN reacts with CO_2 to form Na_2CO_3.

Decay in alkali metal concentration

In an earlier study[15] it was found that both KCN and NaCN vaporize at fairly high rates at temperatures above 900 K. It is also known that when catalytic precursors such as K_2CO_3 and Na_2CO_3 are added to coke, alkali metal vapours are formed during the catalytic gasification process[4].

Several experiments were conducted to determine the extent of potassium loss during the gasification of coke containing KCN, KOCN, K_2CO_3 and NaCN. In each case, a coke sample containing KCN, KOCN, K_2CO_3 or NaCN in the amount of 0.005 kg mol M per kg mol C was gasified in pure CO_2 at 1123 K to different degrees of coke conversion in the range of 0 to 85 % of the initial weight of the sample. The partially reacted samples were then analysed for total potassium or sodium content by atomic absorption spectroscopy.

The results are presented in *Figure 1* as molar M/C ratios measured at various conversions. The decay in the kg mol M/kg mol C ratio in the initial period is indicative of a relatively higher rate of loss of alkali metal than the rate of C gasification. In the subsequent period, as the amount of alkali metal in the coke decreases, the rate of carbon gasification becomes higher than the rate of loss of alkali metal resulting in an increase in kg mol M/kg mol C ratio with the progress of the reaction. The relative
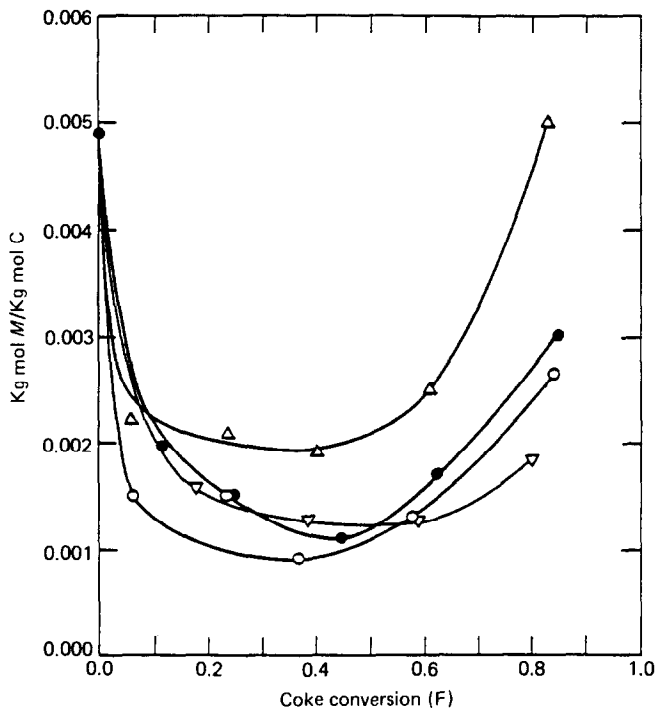
Figure 1 Changes in the concentration of potassium or sodium (*M*) during reaction. $T= 1123$ K; $P_{CO_2} = 101.3$ KPa; initial kg mol M/kg mol C = 0.005. ○, KOCN; ●, KCN; △, K_2CO_3; ▽, NaCN
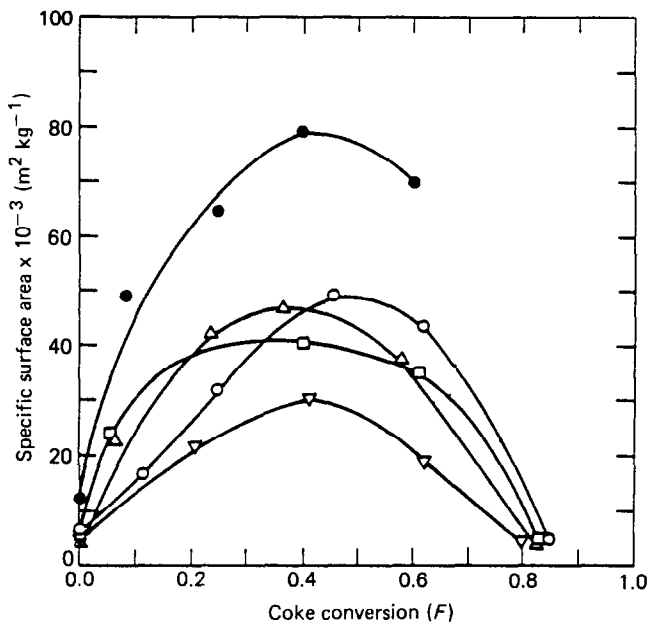
Figure 2 Specific surface area changes during reaction. $T= 1123$ K; $P_{CO_2} = 101.3$ kPa; initial kg mol M/kg mol C = 0.005. ○, KCN; ●, no catalyst; □, K_2CO_3; △, KOCN; ▽, NaCN

changes in the concentration of K and Na depend on several factors such as the relative volatility of K–O–C–N and Na–O–C–N melts, changes in the composition of these melts and their extent of participation in the catalytic process.

Specific surface area

Surface area measurements were carried out on several partially reacted coke samples with or without the addition of catalytic precursors. The initial concentration of the dopant in each case was equal to molar (*M*/C) ratio

of 0.005. The changes in specific surface area of coke after both non-catalysed and catalysed CO_2 gasification as a function of coke conversion are shown in *Figure 2*. The data indicate that at any given conversion, the specific surface areas of coke samples doped with the catalytic precursors are significantly lower than those for the coke sample containing no catalyst. Shadman and co-workers[16] observed a similar behaviour in the KOH catalysed CO_2 gasification of coal char and attributed the decrease in the specific surface area to catalyst induced pore plugging.

The data in *Figure 2* also indicate that the specific surface area of coke samples, with and without the presence of a catalyst, increases with conversion initially, reaches a maximum and decreases towards the end. The figure also indicates that addition of NaCN to coke results in a more significant decrease in surface area of coke compared with KCN addition. This observation is consistent with the relatively more effective coverage of the surface by NaCN resulting from the higher vapour pressure and lower melting temperature of NaCN compared with KCN[17].

Since the addition of alkali metal cyanides reduces the specific surface area, the influence of the concentration of NaCN on the specific surface area was examined. Coke samples were impregnated with various concentrations of NaCN and then heated up to 1123 K in an atmosphere of argon. At this stage, the heating was terminated, the specimens were cooled, and the specific surface area was measured. The results are presented in *Figure 3* as specific surface area *versus* kg mol Na/kg mol C ratio plots. The figure indicates that the addition of a small quantity of NaCN reduces the specific surface area significantly. Since molten NaCN vaporizes at a significant rate at the reaction temperature, the interior of the pores are well covered by the alkali. This extensive surface coverage seems to reduce the specific surface area. However, when the concentration of NaCN in coke is relatively high, addition of further NaCN has a minor effect on the specific surface area.
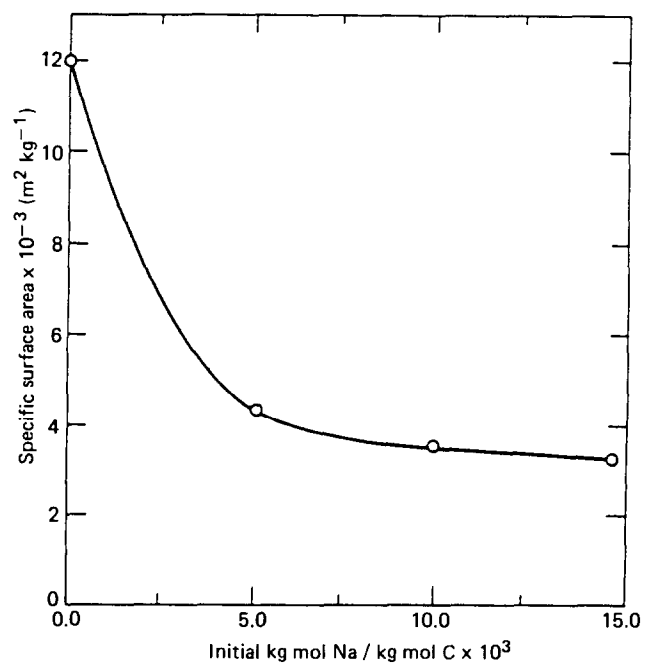
Figure 3 Specific surface area as a function of initial kg mol Na/kg mol C. $T= 1123$ K; $P_{Ar} = 101.3$ kPa; $F= 0.0$. ○, NaCN
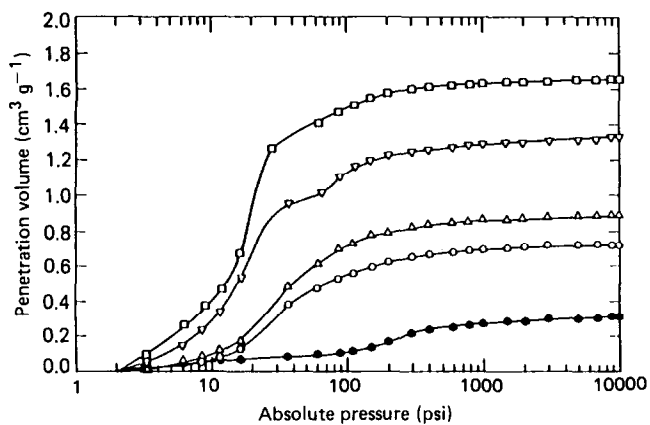
Figure 4 Cumulative pore volume *versus* pore radius plots for partially reacted coke samples doped with NaCN. $T = 1123$ K; $P_{CO_2} = 101.3$ kPa; initial kg mol Na/kg mol C = 0.005. F: ●, 0.00; ○, 0.20; △, 0.40; ▽, 0.59; □, 0.79
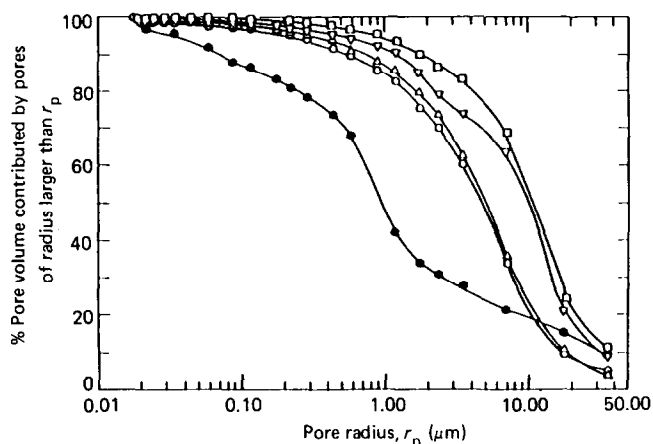
Figure 5 Per cent pore volume contributed by pores of radius larger than r_p *versus* pore radius, r_p, plots for NaCN doped samples. $T = 1123$ K; $P_{CO_2} = 101.3$ kPa; initial kg mol Na/kg mol C = 0.005. F: ●, 0.00; ○, 0.20; △, 0.40; ▽, 0.57; □, 0.79

The variation of surface area with conversion can be explained by the data on pore size distribution studies and by the results of electron microscopy on various partially reacted samples.

Pore size distribution

In *Figure 4*, the extent of mercury penetration in cm^3 g^{-1} is plotted as a function of applied pressure for samples impregnated with NaCN and reacted to various degrees. The data indicate that the pore volume (porosity) increases with the degree of conversion, F. The percentage of the total pore volume contributed by all pores having a radius larger than r_p is plotted against the minimum pore radius, r_p, in *Figure 5*. The data in this figure indicate that the percentage of pore volume contributed by pores of radius 0.1 μm or larger increases with coke conversion in the initial period of reaction. This observation is also true for pores of 1.0 μm or larger. However, when large pores (> 10 μm) are considered, the percentage volume contributed by these pores decreases with increasing conversion up to 40% conversion. Thus, up to 40% conversion, small pores are generated with the progress of the reaction. Beyond 40% conversion, small pores are enlarged and this accounts for the decrease in

the specific surface area. Similar results were obtained for coke samples doped with KCN.

Porosity

The increase in the total porosity of the coke samples doped with NaCN, with conversion, is shown in *Figure 6a*. The contributions of the large (> 10 μm radius) and small pores (< 1.0 μm radius) on the total porosity are indicated in *Figure 6b*. It is seen that the fraction of total porosity due to pores < 1 μm radius decreases with coke conversion. On the other hand, the fraction of porosity due to pores > 10 μm radius remains constant up to $\approx 40\%$ conversion and then increases with conversion. Up to $\approx 40\%$ conversion, the proportion of pore volume contributed by pores having a radius in the range of 1.0 to 10.0 μm increases with conversion, while the contribution of the pores smaller than 1.0 μm radius was diminished with conversion. When the conversion exceeded 40%, the contribution of the pores larger than 10 μm radius to the total porosity increased with conversion.

Microstructures

Microstructures of the fractured surfaces of various partially reacted cokes samples are also consistent with the results of pore size distribution studies by mercury porosimetry. A selection of representative areas of the micrographs for KCN doped samples is presented in *Figure 7a–e*. A comparison of the micrographs 7(a) ($F = 0$, no catalyst) and 7(b) ($F = 0$, kg mol K/kg mol C = 0.005) indicate that the addition of KCN to coke leads to a decrease in the small pores. This fact is in agreement with the observed decrease in specific surface area of the coke
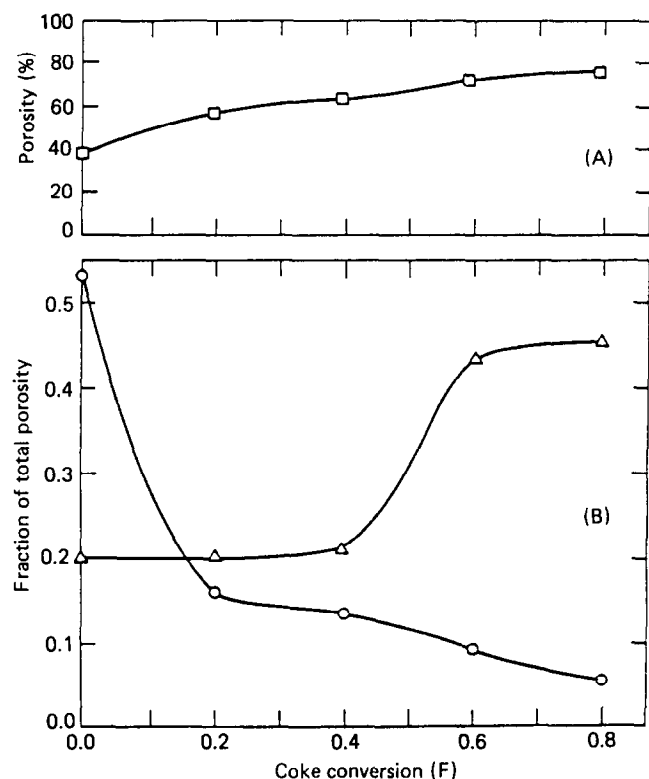
Figure 6 Variation of (A) total porosity, and (B) porosity of coke samples doped with NaCN contributed by pores of a given size range as a function of conversion. $T = 1123$ K; $P_{CO_2} = 101.3$ kPa; initial kg mol Na/kg mol C = 0.005. ○, Fractional porosity due to pores < 1 μm radius; △, fractional porosity due to pores > 10 μm radius
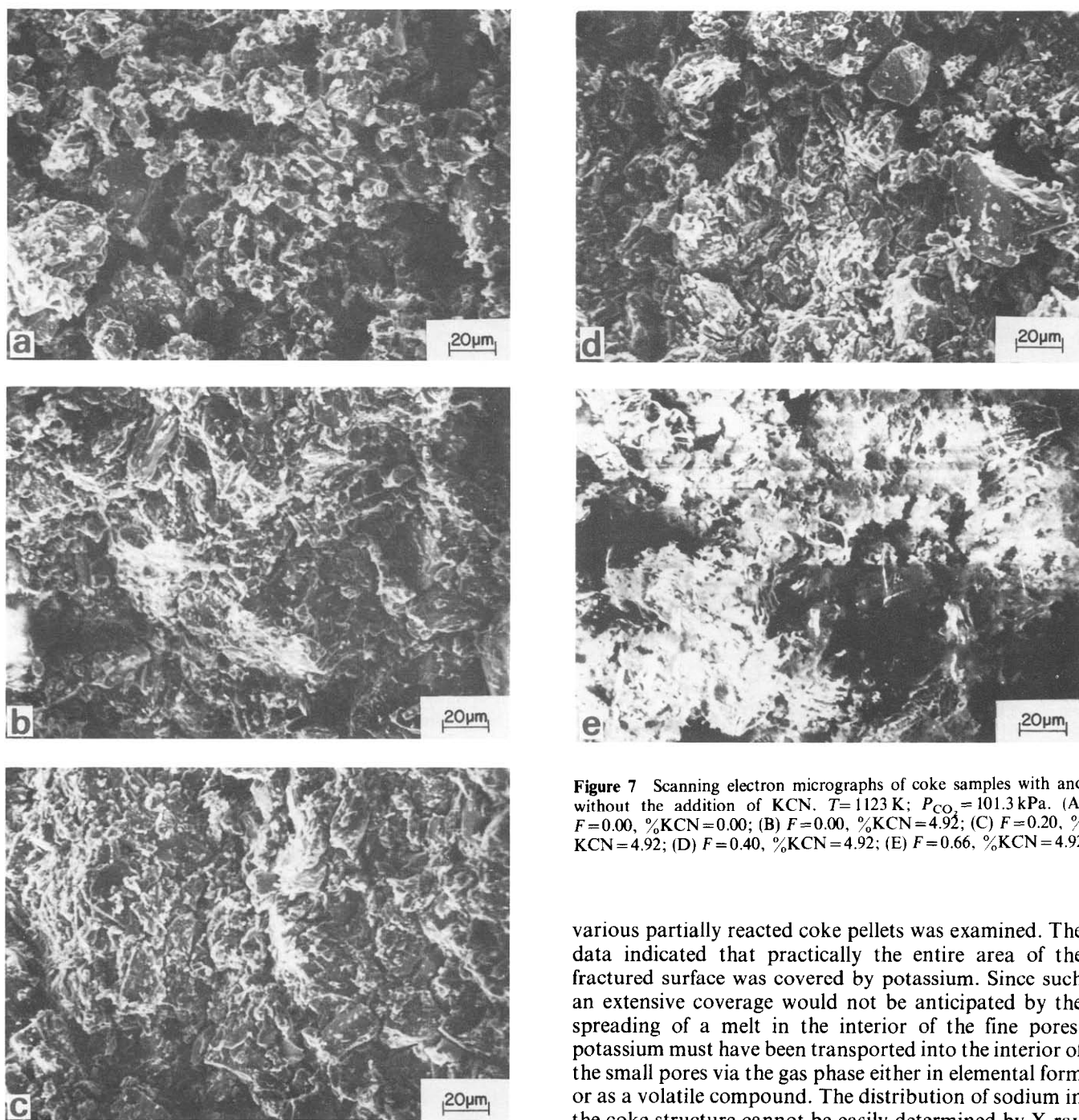
Figure 7 Scanning electron micrographs of coke samples with and without the addition of KCN. $T = 1123$ K; $P_{CO_2} = 101.3$ kPa. (A) $F = 0.00$, %KCN = 0.00; (B) $F = 0.00$, %KCN = 4.92; (C) $F = 0.20$, %KCN = 4.92; (D) $F = 0.40$, %KCN = 4.92; (E) $F = 0.66$, %KCN = 4.92

samples doped with KCN. The effects of the extent of reaction on the pore structure can be observed from *Figures 7b–e*. The presence of small cracks and fissures is apparent in samples reacted up to 40% burn-off (*Figures 7c–d*). The formation of these cracks and fissures leads to the initial increase in the specific surface area at low conversions. At high conversions (*Figure 7e*), relatively large pores are observed in the microstructure. The formation of these large pores is consistent with the decrease in specific surface area at high conversions observed in *Figure 2*.

Distribution of potassium

Since the catalysis of the coke–CO_2 reaction by various precursors depends on the carbon–catalyst contact, the distribution of potassium on the interior surface of various partially reacted coke pellets was examined. The data indicated that practically the entire area of the fractured surface was covered by potassium. Since such an extensive coverage would not be anticipated by the spreading of a melt in the interior of the fine pores, potassium must have been transported into the interior of the small pores via the gas phase either in elemental form or as a volatile compound. The distribution of sodium in the coke structure cannot be easily determined by X-ray studies. However, the distribution of potassium in the coke provides information about the anticipated sodium distribution in the coke.

REACTION KINETICS

Catalytic effects

The rate data for the reaction between coke samples containing various potassium-bearing compounds and CO_2 are presented in *Figure 8* in the form of fractional weight loss, F, versus reaction time, t, plots. The fractional weight loss, F, sometimes referred to as the coke conversion is defined as:

$$F = \triangle W/W_o \qquad (4)$$

where: $\triangle W =$ the weight loss sustained by the sample; and $W_o =$ the initial weight of the coke pellet. For all samples doped with various potassium-bearing precursors, the
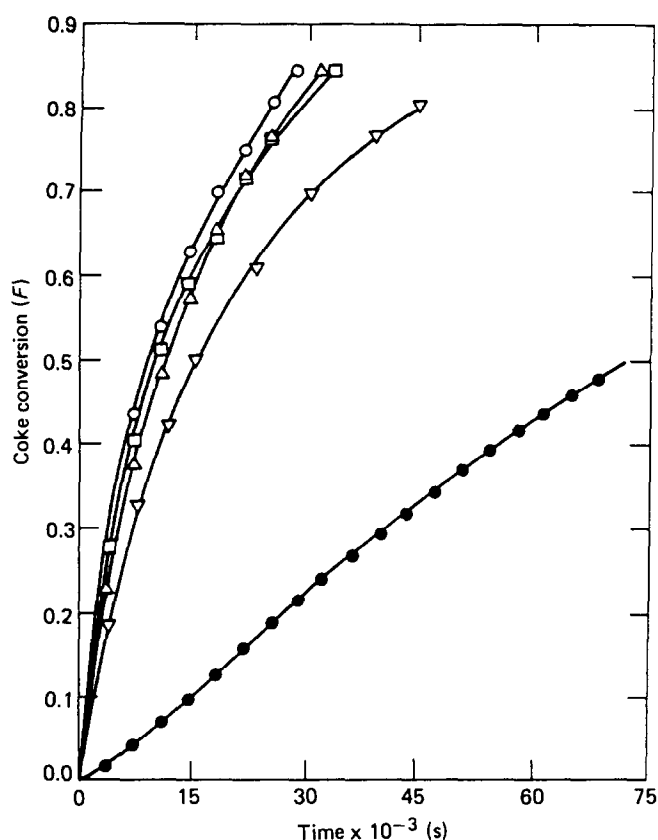
Figure 8 Coke conversion with and without the addition of potassium- and sodium-bearing precursors as a function of time. $T = 1123$ K; $P_{CO_2} = 101.3$ kPa; initial kg mol M/kg mol $C = 0.005$. ●, No catalyst; ○, KCN; □, K_2CO_3; △, KOCN; ▽, NaCN

initial potassium concentrations were maintained constant at a value of kg mol K/kg mol $C = 0.005$.

Two important observation smay be made from the data in *Figure 8*. First, since the addition of potassium-bearing catalytic precursors enhances the rate of coke–CO_2 reaction without significantly influencing the diffusion process, the rate of reaction is not controlled solely by the physical diffusion of gases through the coke structure and through the gas boundary layer. A quantitative assessment of the contribution of the transport steps in the reaction rate is deferred until the end of this section. Second, the data presented in *Figure 8* indicate that for constant potassium loading (kg mol K/kg mol $C = 0.005$), the extent of the enhancement of the rate does not depend on the anionic constituents of the precursors investigated in this study. The similarity in the bahaviour of the precursors can be explained by examination of the mechanism of catalysis. Although it is well known that catalysis by potassium-containing precursors can occur by several mechanisms[2,4,5], the data here can be explained on the basis of the redox mechanism, otherwise known as the vapour cycle mechanism[4]. For an alkali carbonate, M_2CO_3, the steps involved can be represented by the following chemical reactions:

$$M_2CO_3 + 2C = 2M \text{ (g)} + 3CO \tag{5}$$
$$2M\text{(g)} + 2CO_2 = M_2CO_3 + CO \tag{6}$$

$$2C + 2CO_2 = 4CO$$
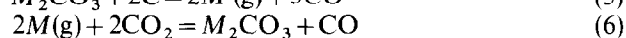
where $M = K$ or Na. Recall that the result of the distribution of potassium in the interior of the coke

samples indicated that potassium was transported inside the coke structure via the vapour phase. The mechanistic scheme described by Reactions (5) and (6) is therefore consistent with the potassium distribution pattern obtained by energy dispersive X-ray studies.

Wet-chemical analysis and X-ray diffraction studies indicated that both KCN and KOCN are partially converted to K_2CO_3 during gasification. The relevant chemical reactions are:

$$2KCN + 4CO_2 = K_2CO_3 + 5CO + N_2 \tag{7}$$
$$2KOCN + 2CO_2 = K_2CO_3 + 3CO + N_2 \tag{8}$$
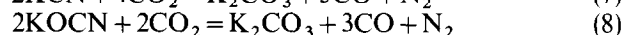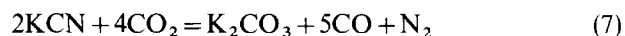
Following the generation of K_2CO_3, the catalysis can then proceed via Reactions (5) and (6) when KCN or KOCN are used as catalytic precursors.

The relative influence of KCN and NaCN on the enhancement of the rate of CO_2 gasification of coke is also presented in *Figure 8*. The data indicate that KCN enhances the rate more than NaCN. This observation can be explained on the basis of the redox mechanism[4]. The steps involved in the mechanistic scheme are presented by Reactions (5) and (6). The presence of an adequate amount of metal vapour is central to the catalytic process. Therefore, in Reaction (5), the equilibrium partial pressures of K and Na vapours can give some idea about the relative effectiveness of K and Na as catalytic precursors.

From the available thermodynamic data[17], the equilibrium pressures of K(g) and Na(g) were calculated at several P_{CO} values for the experimental conditions and the results are presented in *Table 2*. The data indicate that the equilibrium partial pressure of K is higher than that of Na. The calculated vapour pressures of K and Na are therefore consistent with the realtive catalytic effects of KCN and NaCN observed in *Figure 8*.

Reaction rate measurements were also carried out at various partial pressures of CO and CO_2 to determine whether the influence of the partial pressures of these gases on the reaction rate can be explained on the basis of the redox mechanism. For coke samples doped with KCN and NaCN, the data are presented in *Figure 9*. The figure indicates that the addition of CO significantly retards the rate of the coke–CO_2 reaction in the presence of KCN and NaCN. Also, the partial pressure of CO_2 influences the reaction rate. These observations are in agreement with the importance of Reactions (5) and (6) in determining the overall rate.

Effects of K and Na concentrations and specific surface area

Unless the diffusion of CO and CO_2 through the pore structure of the coke is slower than the rate of reaction of

Table 2 Equilibrium pressures of K(g) and Na(g) at 1123 K and different P_{CO} values

P_{CO} (kPa)	$P \times 10^5$ (kPa) calculated from Reaction (5)	
	Na	K
10.1	0.070	0.175
20.2	0.025	0.062
40.5	0.009	0.022
60.8	0.005	0.012
81.0	0.003	0.008
91.2	0.002	0.006
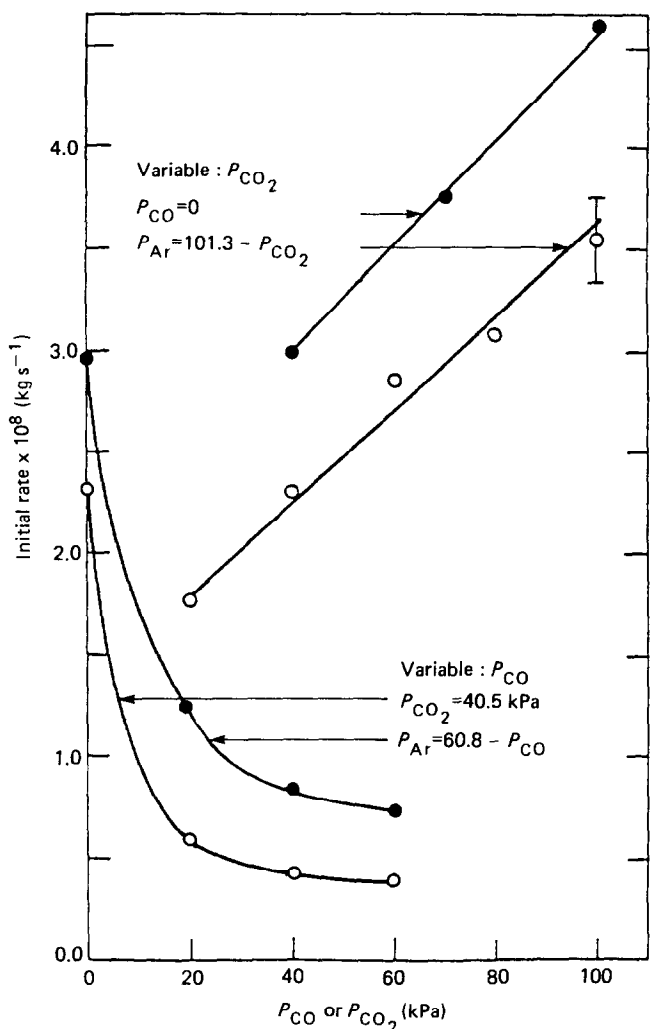
Figure 9 Effects of the partial pressures of CO and CO_2 on the rate of coke–CO_2 reaction in the presence of alkali metal cyanides. T= 1123 K; initial kg mol M/kg mol C = 0.005. ○, NaCN; ●, KCN

in kg C/kg mol M-s, is plotted as a function of the conversion, F, in *Figure 12*. The trends of the initial increase and the subsequent decay of the reaction rate, again, are similar to the changes in the specific surface area presented in *Figure 2*. Thus, if the changes in the catalyst concentration are decoupled from the rate data, the influence of the specific surface area on the reaction rate becomes apparent.

The effects of variables other than specific surface area and the concentration of the catalyst can be measured by examining the rate per unit surface area per unit concentration of the catalyst (*Figure 13*). The changes in the reaction rate as a function of conversion can be attributed to various other factors including porosity, pore size distribution and the concentration of active sites. Of these factors, the contribution of the pore
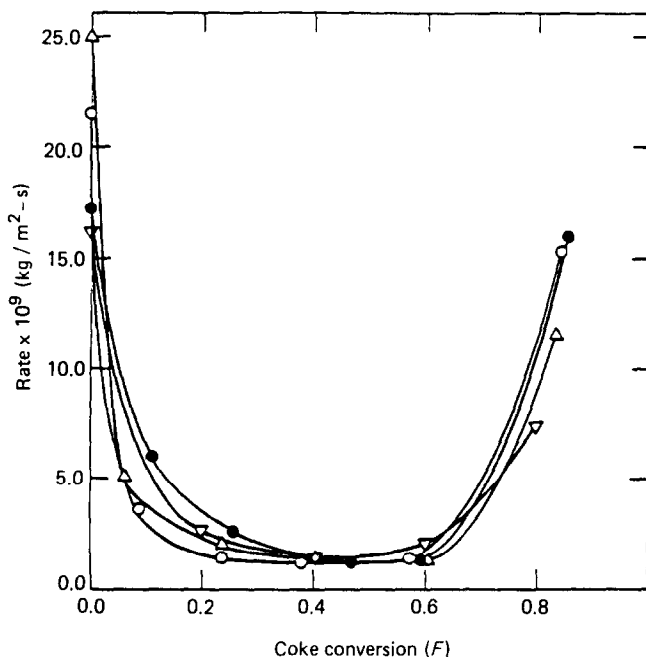
Figure 10 Rate per unit surface *versus* coke conversion. T= 1123 K; P_{CO_2} = 101.3 kPa; initial kg mol M/kg mol C = 0.005. ●, KCN: ○, KOCN: △, K_2CO_3; ▽, NaCN

CO_2, both the specific surface area of the coke and the catalyst concentration should have appreciable effects on the reaction rate. To decouple the rate data from the geometrical effects of the specific surface area changes during the reaction, the reaction rate per unit surface area is plotted as a function of coke conversion, F, in *Figure 10*. The rate per unit area decreased initially with conversion, remained fairly constant up to about F = 0.6 and then increased. The shape of these plots resembles the shape of the (kg mol M/kg mol C) *versus* coke conversion plots presented in *Figure 1* for various catalytic precursors. Therefore, it seems that once the geometrical effect of the surface area changes were eliminated from the rate data, the variation in reaction rate appeared to be similar in nature to the variation in the concentration of alkali metal. In fact, when the initial rates of coke samples doped with various concentrations of potassium and sodium are plotted as a function of the concentration of potassium and sodium, and the structural effects are eliminated to a large extent, the rate seems to be influenced by the concentration of alkali metal (*Figure 11*).

Again, the rate data can be decoupled from the effects of potassium and sodium concentration changes by dividing the rate by the instantaneous concentration of potassium or sodium. The reaction rate thus obtained (i.e., based on a constant alkali metal amount), expressed

Figure 11 Initial gasification rate as a function of initial concentration of alkali metal in coke pellet. T= 1123 K; P_{CO_2} = 101.3 kPa. ○, NaCN; ●, KCN
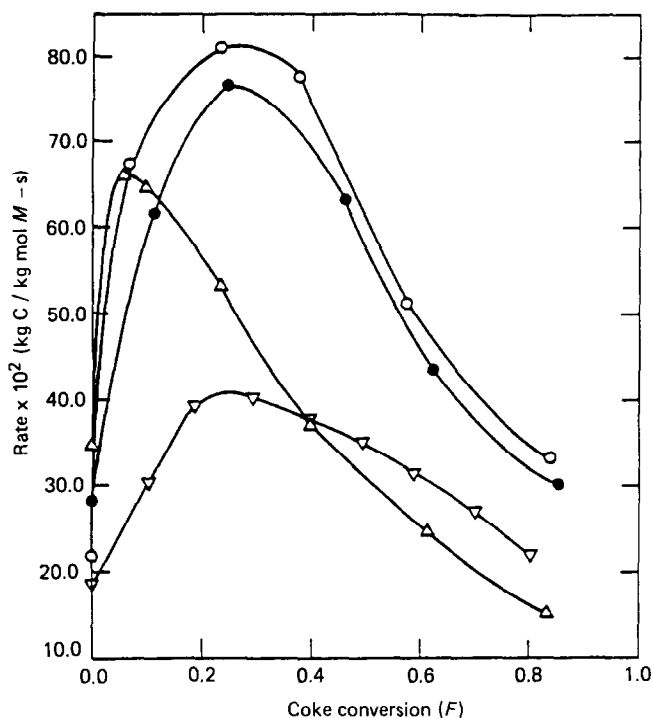
Figure 12 Rate per unit amount of alkali metal *versus* conversion. $T = 1123$ K; $P_{CO_2} = 101.3$ kPa; initial kg mol M/kg mol $C = 0.005$. $\bigcirc$, KOCN; $\bullet$, KCN; $\triangle$, K_2CO_3; $\triangledown$, NaCN

diffusion to the overall rate can be assessed by examining the values of the effectiveness factor, η, defined as the ratio of the measured reaction rate to the intrinsic reaction rate. The procedure is described below.

Role of pore diffusion

The effectiveness factor, η, is expressed as:

$$\eta = \frac{S_p J_a}{K_v(P - P_e)V_p} \tag{9}$$

where:

S_p = external surface area of the coke pellet (m^2)
J_a = measured reaction rate (kg mol/m^2 − s)
K_v = intrinsic reaction rate constant (kg mol s/m^2 kg)
P = partial pressure of CO_2 at a distance x from the surface of the pellet (kg/m − s^2)
P_e = equilibrium pressure of CO_2 (kg/m − s^2)
V_p = volume of the coke pellet in m^3

The equation for the conservation of CO_2 assuming quasi steady state and first order reaction is given by[5]:

$$\frac{D_e}{RT}\frac{d^2 P}{dx^2} - K_v (P - P_e) = 0 \tag{10}$$

where: D_e = effective diffusivity of CO_2 (m^2 s^{-1}); R = gas constant = 9.314×10^3 kg − m^2/s^2 − kg mol − K; and T = temperature (K).

The above equation is solved using the following boundary conditions:

$$P = P_s \quad \text{at } x = 0 \tag{11a}$$

$$\frac{dP}{dx} = 0 \quad \text{at } x = L \tag{11b}$$

where: P_s = partial pressure of CO_2 at the pellet surface (kg/m − s^2); L = characteristic length of the pellet (m).

For the disc-shaped pellets the characteristic length, L, which is also the effective diffusion distance, was calculated by dividing the pellet volume with the total external surface area of the pellet. It was found that the calculated value of L works out to be smaller than 50% of the pellet thickness. This value reflects augmentation of the diffusion through the flat surfaces by the contribution of diffusion through the curved cyrlindrical surface of the pellet. Such a procedure for the computation of the effective diffusion distance was adopted in several previous investigations[5,18−21]. The equation of conservation of CO_2 at the surface of the pellet is given by:

$$K_g (P_b - P_s) = -D_e\left(\frac{dP}{dx}\right)_{x=0} \tag{12}$$

where: K_g = gas phase mass transfer coefficient in m s^{-1}; P_b = partial pressure of CO_2 in the bulk phase in kg/m − s^2.

The gas phase mass transfer coefficient, K_g, was calculated by using an appropriate mass transfer correlation available in the literature[22]. The following intermediate variable is introduced to aid in the solution:

$$\phi = L\sqrt{\frac{K_v RT}{D_e}} \tag{13}$$

A solution to Equations (9)–(13) can be expressed in terms of the dimensionless parameter, ϕ, as[5]:

$$\frac{1}{K_g} + \frac{L \coth\phi}{\phi D_e} = \frac{(P_b - P_e)}{J_a RT} \tag{14}$$

It may be observed that from the knowledge of ϕ, the value of the intrinsic reaction rate constant, K_v, can be readily obtained from Equation (13). An expression for the effectiveness factor, η, can be derived from the solution of the above set of equations as[5]:

$$\eta = \frac{1}{K_v RTL\left(\dfrac{1}{K_g} + \dfrac{L\coth\phi}{\phi D_e}\right)} \tag{15}$$

Therefore, from the knowledge of L, K_g, D_e, K_v and ϕ, the value of the effectiveness factor, η, can be readily determined. Since the pore size distribution changes significantly with the reaction time, the value of the effective diffusivity, D_e, must be computed as a function of
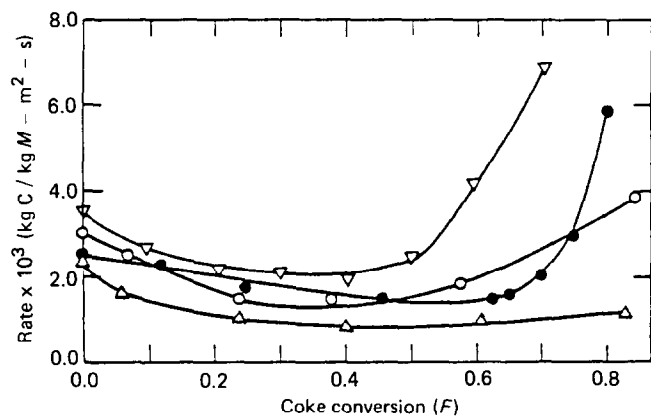
Figure 13 Rate per unit surface area per unit weight of alkali metal *versus* conversion. $T = 1123$ K; $P_{CO_2} = 101.3$ kPa; initial kg mol M/kg mol $C = 0.005$. $\bullet$, KCN; $\bigcirc$, KOCN; $\triangle$, K_2CO_3; $\triangledown$, NaCN

reaction time. For the calculations reported here, the value of the mean pore size, $\bar{r}$, was determined from the results of the mercury penetration porosimetry at various coke conversions.

For coke samples doped with KCN and NaCN, values of the effectiveness factor, η, are presented in *Figure 14* as
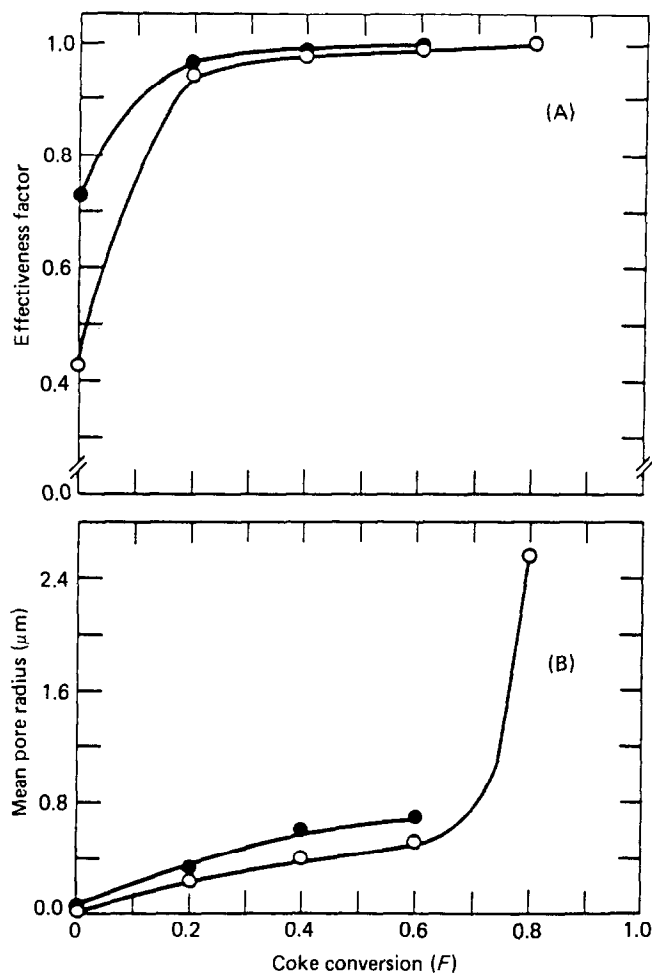
Figure 14 (A) Effectiveness factor, and (B) mean pore size of KCN and NaCN doped samples as a function of coke conversion. $T = 1123$ K; $P_{CO_2} = 101.3$ kPa; initial kg mol K/kg mol C = 0.005. ○, NaCN; ●, KCN

a function of coke conversion, F. The values of the mean pore radius required for the calculation of the effective diffusivity values obtained from the mercury porosimetry data are also presented in the same diagram. The data for the calculation of η are presented in *Table 3*. The value of $\bar{r}$ is assumed to be 33 % of the average pore radius following the recommendation by Satterfield[23]. The computed values of η indicate that at low conversions, when the mean pore size is rather small, the rate of the catalytic reaction is influenced, in part, by the diffusion of CO_2 through the porous coke. However, as the pores are enlarged due to reaction, the pore diffusion is increasingly facilitated and at high conversion values the rate is controlled solely by the chemical reaction. *Figure 14* also indicates that at low conversions the rate is influenced more significantly by the diffusion process for coke samples doped with NaCN as compared to coke samples doped with KCN. This is consistent with the fact that NaCN doped samples have a smaller mean pore radius as compared to KCN doped samples.

CONCLUSIONS

During the gasification of coke doped with MCN or KOCN, a melt containing K, C, O and N is formed that contains at least one anion other than the dopant anion. KCN, KOCN and K_2CO_3 enhanced the rate of the reaction equally. Similarly, when coke specimens doped with NaCN are gasified in CO_2, a melt containing Na, C, O and N is formed which on cooling precipitates NaCN, NaOCN and Na_2CO_3. At the reaction temperature, potassium and sodium-bearing melts act as effective agents for the catalysis of the coke–CO_2 reaction.

The concentrations of potassium and sodium in the coke sample change significantly with the progress of the reaction. An examination of the distribution of potassium in the interior of coke using the energy dispersion X-ray technique revealed extensive coverage of the interior surface of coke by potassium. Such an extensive coverage is possibly one if potassium is transported in the interior of coke via the gas phase.

The addition of alkali-bearing compounds to coke resulted in a decrease in the specific surface area of coke because of the deposition of alkalis in the interior of the

Table 3 Data for the calculation of effectiveness factor

Conversion (F)	Porosity (%) (θ)		Mean pore radius ($\bar{r}$) (μm)		Rate × 10⁵ (kg mol/m² – s)	
	KCN	NaCN	KCN	NaCN	KCN	NaCN
0.0	40.4	37.4	0.06	0.015	2.42	1.73
0.2	48.4	56.4	0.28	0.23	1.64	1.02
0.4	54.2	62.2	0.59	0.40	0.84	0.61
0.6	58.1	70.9	0.68	0.50	0.45	0.36
0.8	–	75.2	–	2.56	–	0.16

Temperature (T), 1123 K; Partial pressure of CO_2 in the bulk gas stream (P_b), 1.01×10^5 kg/m–s²; Equilibrium pressure of CO_2 (P_e), 0.073×10^5 kg/m–s²; Pellet diameter (d_p), 9.5×10^{-3} m; Pellet thickness (t_p), 4.7×10^{-3} m; Characteristic length of pellet (L), 1.18×10^{-3} m; Gas constant (R), 8314 kg–m²/kg mol–s²–K; Gas phase mass transfer coefficient (K_g), 4.90×10^{-2} m s⁻¹; Binary diffusivity of CO and CO_2 (D_b), 1.52×10^{-4} m² s⁻¹; Effective diffusivity of CO_2, $D_e = \dfrac{\theta^2 D}{\sqrt{3}}$ (m² s⁻¹); Diffusivity of $CO_2 = D = \left(\dfrac{1}{D_b} + \dfrac{1}{D_k}\right)^{-1}$ (m² s⁻¹); Knudsen diffusivity of CO_2,

$$D_k = \tfrac{2}{3}\bar{r}\sqrt{\frac{8RT}{\pi M}} \ (\text{m}^2\text{s}^{-1})$$

pores. Addition of KCN caused a somewhat less extensive reduction in the specific surface area compared with NaCN. This is consistent with the relatively low vapour pressure and higher melting point of KCN than NaCN. The changes in the specific surface area with conversion were not affected by the anionic component of the potassium-bearing precursors investigated.

During gasification, the specific surface area increases in the initial period reaches a peak and then decreases. The changes in the specific surface area during reaction can be explained by the changes in the pore size distribution of the coke. The initial increase in the surface area is attributed to the generation of small pores, whereas the decrease in the surface area at high conversions is caused by the enlargement of the pores.

Although the specific surface area of the partially reacted coke containing no catalyst is higher than the specific surface area of the coke containing various precursors, the way in which the specific surface area changes with burn-off is similar in both cases. The catalytic effect of KCN is found to be more pronounced than that of NaCN. This difference is consistent with the higher equilibrium vapour pressure of K(g) than that of Na(g). The catalytic effects of the precursors could be explained by the redox mechanism.

When the effects of the changes of specific surface area and the concentration of alkali metal were decoupled from the rate, the reaction rate (kg mol C/kg mol M-m^2-s) was found to be relatively insensitive to the extent of reaction. Thus, changes in specific surface area and the concentration of alkali metal are the most dominant factors in determining the rate of the catalysed reaction.

During the initial stages of the reaction when the average pore radius is small, the computed values of the effectiveness factor are 0.43 and 0.72 for coke samples doped with NaCN and KCN, respectively. This indicates that the overall gasification rate is influenced, in part, by the diffusion of CO_2 through the porous coke during the initial stages. At later stages of the reaction, when the conversion is $> 20\%$, the computed effectiveness factor values for samples doped with KCN and NaCN are > 0.9 and the rates in both cases are controlled by the chemical reaction between coke and CO_2.

REFERENCES

1 Walker, P. L., Jr., Shelf, M. and Anderson, R. 'Chemistry and Physics of Carbon', (Ed. P. L. Walker, Jr.), Vol 4, Edward Arnold, London, 1968, p. 287
2 Wen, W. Y. Catal. Rev. Sci. Eng. 1980, 22, 1
3 McKee, D. W. 'Chemistry and Physics of Carbon', (Eds. P. L. Walker, Jr. and P. A. Thrower), Vol 16, Marcel Dekker, New York, 1981, p. 1
4 McKee, D. W. and Chatterji, D. Carbon 1978, 16, 53
5 Rao, Y. K. and Jalan, B. P. Carbon 1978, 16, 175
6 Veera, M. J. and Bell, A. T. Fuel 1978, 57, 194
7 Mims, C. A. and Pabst, J. K. Am. Chem. Soc., Div. Fuel Chem., Prepr. 1980, 25(3), 258
8 Sams, D. A. and Shadman, F. Fuel 1983, 62, 880
9 Alam, M. and DebRoy, T. Ironmaking and Steelmaking 1985, 12(5), 203
10 Alam, M. and DebRoy, T. Metal. Trans., B. 1986, 17B, 565
11 Wigman, T., Hoogland, A., Tromp, P. and Moulijn, J. A. Carbon 1983, 21, 13
12 Alam, M. and DebRoy, T. Metal. Trans. 1984, 15B, 400
13 Alam, M. and DebRoy, T. ISS Trans. 1984, 4, 7
14 Thompson, R. P., Mantione, A. F. and Aikman, R. P. Blast Furnace and Steel Plant 1971, 59, 161
15 Alam, M. and DebRoy, T. ISS Trans. 1985, 6, 15
16 Hamilton, R. T., Sams, D. A. and Shadman, F. Fuel 1984, 63, 1008
17 'JANAF Thermochemical Tables', 2nd Ed., US Government Printing Office Washing, DC, 1971
18 Roberts, G. W. and Satterfield, C. N. Ind. Eng. Chem. Fundam. 1965, 4, 288
19 Aderibigbe, D. A. and Szekely, J. Ironmaking and Steelmaking 1982, 9(1), 33
20 Rao, Y. K. and Jalan, B. P. Metal. Trans. 1972, 3, 2465
21 Aris, R. Chem. Eng. Sci. 1956, 6, 282
22 Turkdogan, E. T. 'Physical Chemistry of High Temperature Technology', Academic Press, New York, 1980
23 Satterfield, C. N. 'Mass Transfer in Heterogeneous Catalysis', MIT Press, Cambridge MA, 1970